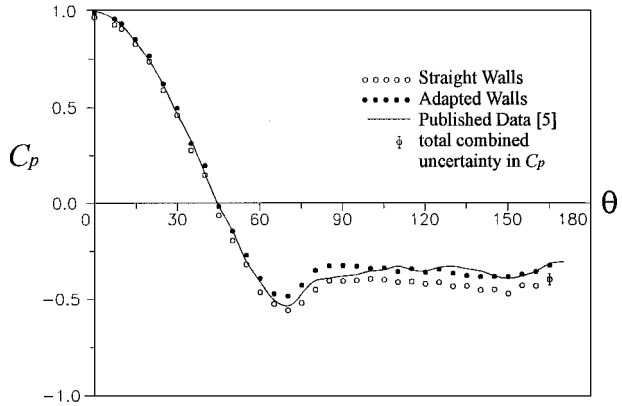

Fig. 2 Sphere surface static pressure distributions ($\phi = 0$ deg) with the sphere positioned on the test section centerline ($c/b = 0.5$), at $Re_d = 1.69 \times 10^5$, illustrating the effectiveness of the two-dimensional wall adaptation in removing the effects of wall interference. The total combined uncertainty is estimated at $C_p \pm 0.03$.

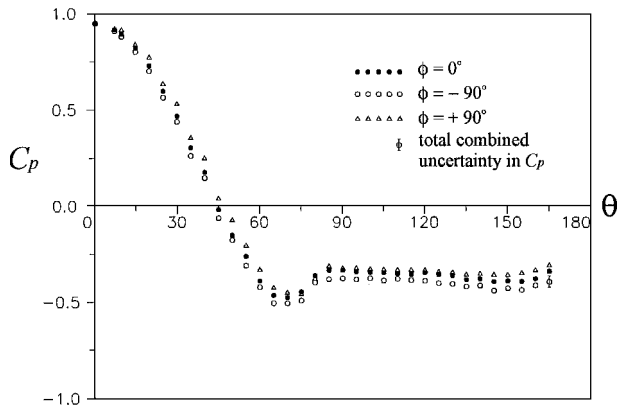

Fig. 3 Mean static pressure distributions at $c/b = 0.2$ and $Re_d = 1.69 \times 10^5$ for adapted walls. Two-dimensional wall adaptation provided a correction to the base pressure region but could not correct the asymmetrical nature of the flowfield about the sphere at this cross-stream position (total combined uncertainty of $C_p \pm 0.03$).

the $C_p(\theta)$ distribution and C_D (Table 1). The flow pattern, however, remained asymmetric (Fig 3).

Permissible Range for Cross-Stream Position

The permissible range for cross-stream position of the center of the sphere extends from the test section longitudinal centerline to a distance of $0.2b$ (121.9 mm) toward either side wall. Since the sphere has a radius of 63.5 mm ($0.10b$), the permissible range for model lateral position extends $\pm 0.3b$ from the centerline. Since a similar extension of the permissible working zone can also be accommodated in the vertical direction, through adjustment of the roof and floor contours,[3] a conservative estimate is placed on the permissible zone in which three-dimensional models such as a sphere can be located: it is assumed that the model must be located within a circle of radius $0.3b$, centered on the test section centerline. Thus the permissible test zone in which a sphere of 3.6% solid blockage can be placed is the central 28% of the test section cross-sectional area.

Conclusions

The experimental results lend further support to the careful use of a two-dimensional wall adjustment strategy for low-speed, three-dimensional flows under specific conditions for solid blockage of less than 4% for semiaerodynamic shapes, model span in the cross-stream direction of up to 20%, and model proximity to the side walls of $c/b \geq 0.3$. This result yields a permissible test zone comprising 28% of the test section area. The experiments also demonstrate that three-dimensional models such as a sphere can be tested in an environment of minimum wall interference without the need to employ a more computationally intensive and instrumentation-demanding three-dimensional wall adjustment strategy.

References

[1] Sumner, D., "An Experimental Investigation of Three-Dimensional Models in a Two-Dimensional Adaptive Wall Test Section," M.A.Sc. Thesis, Dept. of Mechanical Engineering, Univ. of Waterloo, ON, Canada, 1994.

[2] Sumner, D., and Brundrett, E., "Testing Three-Dimensional Bluff-Body Models in a Low-Speed Two-Dimensional Adaptive Wall Test Section," *Journal of Fluids Engineering*, Vol. 117, 1995, pp. 546–551.

[3] Kankainen, P., Brundrett, E., and Kaiser, J. A., "A Small Wind Tunnel Significantly Improved by a Multi-Purpose, Two-Flexible-Wall Test Section," *Journal of Fluids Engineering*, Vol. 116, 1994, pp. 419–423.

[4] Wolf, S. W. D., and Goodyer, M. J., "Predictive Wall Adjustment Strategy for Two-Dimensional Flexible Walled Adaptive Wind Tunnel—A Detailed Description of the First One-Step Method," NASA CR 181635, 1988.

[5] Achenbach, E., "Experiments on the Flow Past Spheres at Very High Reynolds Numbers," *Journal of Fluid Mechanics*, Vol. 54, Pt. 3, 1972, pp. 565–575.

R. W. Wlezien
Associate Editor

Near-Field Experiments on Tip Vortices at Mach 3.1

Frank Y. Wang* and Pasquale M. Sforza†
Polytechnic University, Brooklyn, New York 11201

Introduction

LIMITED experimental investigations of the supersonic flowfield behind low aspect ratio, unswept wings were conducted over four decades ago by Davis[1] and Adamson and Boatright.[2] Recently, pitot measurements of supersonic tip vortices from different unswept wings were made by Kalkhoran et al.,[3] Wang and Sforza,[4] and Wang.[5] Most recently, Smart et al.[6] made additional measurements in such flows using pitot and cone probes. This limited database prompted the present Note, which expands upon the key features of the previous findings. The tip vortex generator used is a straight half-wing with a modified double wedge airfoil and a 45-deg chamfer at the tip. It has a chord of 76.2 mm, a thickness of 7.9 mm, a span of 118.75 mm, and a half-wedge angle of 8.3 deg. The tests were made in a Mach 3.1 stream (25.4 × 26.2 cm tunnel cross section) at a Reynolds number of 7.08×10^6 based on the chord for two angles of attack.

Results and Discussion

Previous experience indicates that the diameter of the vortex core (defined as the distance between the swirl velocity peaks) is well represented by the size of the darker band trailing off the wingtip in shadowgraphs.[5] Core diameters, thus, were measured off shadowgraphs taken during the study,[4,5] resulting in values of 6.4 ± 0.8 and 8.5 ± 0.8 mm for $\alpha = 5$ and 10 deg, respectively. These shadowgraphs show virtually no change in the size of the core within the near-field viewing area. This suggests that the radial velocity component is small compared to the axial component and the effect of diffusion is minor, analogous to features found in the incompressible counterpart. Vortex locations were determined using a traversable pitot rake positioned horizontally across the tunnel centerline. Pitot pressure measurements (uncertainty of ± 1.86 kPa) were made at 2.3 chords downstream of the trailing edge for $\alpha = 5$ and 10 deg. This survey location was well within the region free of reflections of the wing's shock-expansion patterns. Pitot pressure results were

Received May 28, 1996; revision received Dec. 6, 1996; accepted for publication Jan. 28, 1997.

*Research Engineer, Department of Mechanical, Aerospace, and Manufacturing Engineering; currently National Science Foundation International Fellow, von Kármán Institute for Fluid Dynamics, 72 Chaussée de Waterloo, B-1640 Rhode-St-Genèse, Belgium. Member AIAA.

†Professor, Department of Mechanical, Aerospace and Manufacturing Engineering. Associate Fellow AIAA.

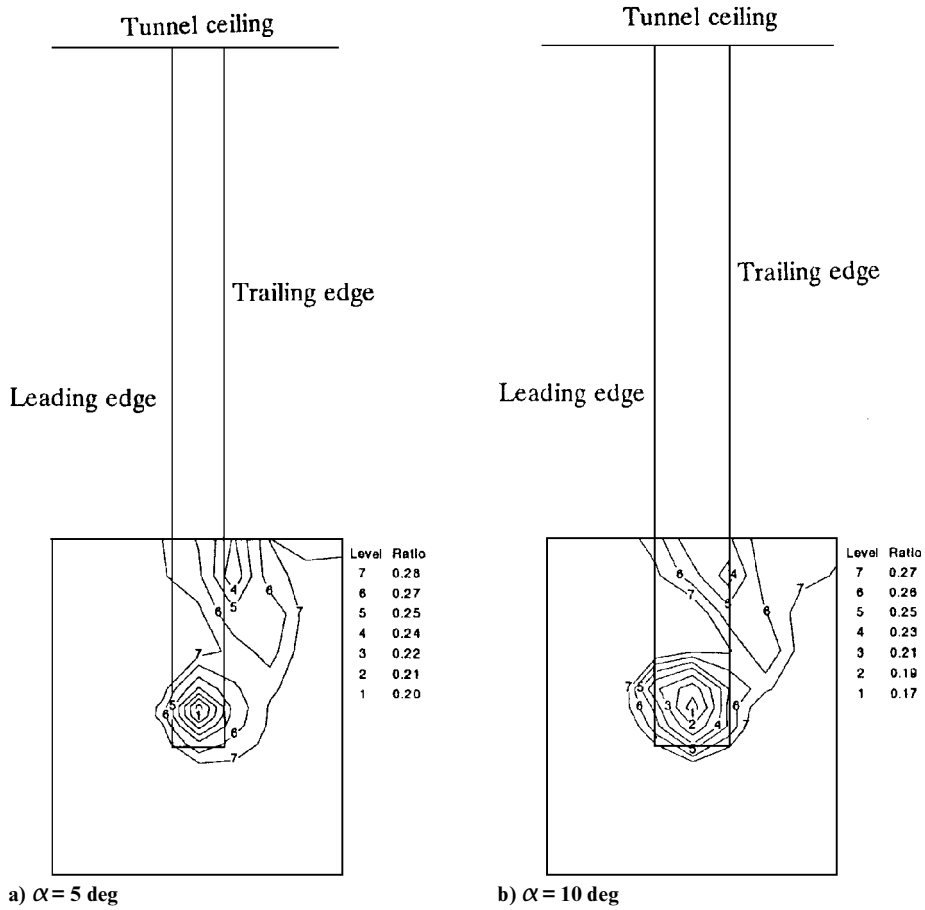

Fig. 1 Pitot pressure contours shown to scale; boxed region outlines survey limits and projection of wing on the measurement plane is superimposed for reference.

normalized by the stagnation pressure (1.17 MPa) and are presented in Fig. 1. The surveys had a constant horizontal spatial resolution of 6.4 mm and a variable vertical spatial resolution as small as 1.6 mm in the vicinity of the core centers. Previous works[5,6] point out that the locations of minimum pitot pressure and of zero swirl in the vortex are approximately the same. The vortex core centers, therefore, are considered to be located by the minimum pitot readings for the surveys conducted. Figure 1 reveals that the trailing vortices drifted slightly inboard at the surveyed station but displayed no downwash for both angles of attack tested. Similar vortex locations were also reported in Refs. 1 and 2. It was noticed that for the $\alpha = 10$ deg case, introduction of a probe into the core center caused the vortex to burst sporadically, events which did not occur in the $\alpha = 5$ deg survey. Conditional sampling, achieved by temporal correlation of the spark discharge of the shadowgraph light source and the pressure transducer signals, was used to extract the unburst portion of the pitot pressure record.

A rake of seven common stainless-steel sewing needles was positioned vertically across the vortex core locations. Shadowgraphs of the weak waves generated provide an estimate of the transverse distribution of the axial Mach number.[5] Close examination of the negatives under maximum magnification showed all of the waves to be unrefracted and essentially equivalent in angle. The tip vortex, therefore, may be said to have an approximately uniform axial Mach number distribution of 3.1, within the photographic resolution. If there were a large axial Mach number gradient in the cores, the waves would have exhibited clear signs of refraction. The uncertainty in measuring the wave angles is ± 1 deg, bounding the axial Mach number in the core between 3 and 3.3, a deviation which amounts to from -3 to $+6\%$ of the freestream value. Results for pitot pressures measured vertically through the vortex center normalized with the freestream pitot pressure are presented in Fig. 2. With the approximations of constant Mach number and stagnation

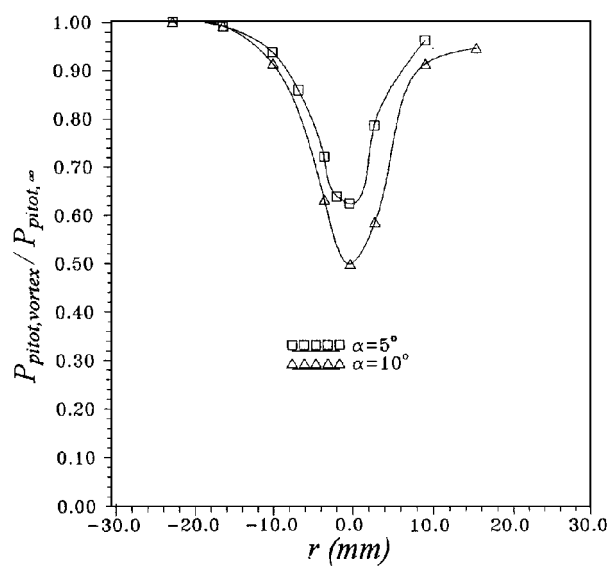

Fig. 2 Normalized pitot pressure profiles.

temperature, the same profiles can also be interpreted as stagnation pressure, static pressure, and density profiles normalized by their respective freestream values. The implication of essentially constant axial Mach number and stagnation temperature is that static temperature and axial velocity are also nearly constant across the vortices.

Low-speed tip vortex experiments have shown axial velocity profiles to span the range from wakelike, to uniform, to jetlike behavior. During the generation of the vortex, the axial flow is retarded by losses resulting from crossflow separation around the tip and propelled at the same time by the circulation. Assuming a polytropic

process in the core, and following the arguments of Batchelor,[7] the axial Mach number in the compressible vortex core becomes

$$\frac{M_x^2}{1+0.5(\gamma-1)M_x^2}=\frac{1}{\gamma RT_0}\left\{V_\infty^2+\left[7\left(\frac{n-1}{n}\right)-2\right]\right.$$

$$\left.\times\int_r^{r_{\text{core}}}\frac{C^2}{r^3}\,\mathrm{d}r+\int_r^{r_{\text{core}}}\frac{1}{r^2}\frac{\partial C^2}{\partial r}\,\mathrm{d}r-2\Delta H\right\} \tag{1}$$

where n is the polytropic exponent, $C \equiv rw$ (w is the swirl), T_0 is the stagnation temperature, and ΔH is the change in stagnation enthalpy between the freestream and the core flows. The two integrals involving C result from relating the pressure gradient within the vortex to the circulation. For a reasonable swirl profile in the core, such as rigid-body rotation, the net contribution from the two integrals involving C is positive. Therefore, the circulation and losses influence the axial flow within the compressible vortex core in the same manner as they do in incompressible cases. When the swirl induced pressure deficit is strong enough, the axial Mach number develops a jetlike profile despite losses arising from crossflow separation around the tip. In high-speed flows over slender bodies with limited heat transfer or viscous effects, the term ΔH is typically small. Therefore, it appears likely that a jetlike axial Mach number profile exists in the core of a tip vortex of a slender supersonic wing, at least in the near field. The maximum magnitude of the jetlike Mach number profile for the current experimental arrangement may be estimated from Eq. (1) by considering an inviscid isentropic flow with a rigid-body rotation swirl profile in the core and assuming that the vortex circulation stems from the entire lift produced in the wing tip region. Such an idealized assessment yields an axial Mach number of 3.26 in the vortex core, which represents only a 5% overshoot (for $\alpha = 10$ deg); any actual overshoot should be smaller. Note that this estimated Mach number of 3.26 falls within the range of the uncertainty in reading the wave angles.

When the wing tip airfoil section is thin[1,2] or chamfered to a sharp edge (the present case), the evidence indicates that there is no appreciable axial Mach number deficiency. However, when the airfoil is much thicker and the tip is squared off, a pronounced Mach number deficit is observed.[6] It is suggested that the crossflow separation around a thick and squared-off tip produces losses sufficient to result in an axial Mach number deficit in the core in the near field. A recent numerical investigation of supersonic wingtip vortices was performed by Rizzetta[8] for conditions corresponding to the experiments of Smart et al.[6] Although the computations underpredict the extent of the axial Mach number deficits reported experimentally, it is evident that increasing the magnitude of the viscous effect results in correspondingly increased axial Mach number deficits in the core. This suggests that a wing with a thin or chamfered tip is less likely than one with a thick and squared-off tip to produce a wakelike axial flow profile in the core because the losses produced by the crossflow separation during vortex generation are smaller. In many respects this is analogous to the formation of a leading-edge vortex from a sharp edged delta wing in which little viscous fluid is entrained in the core[8] and a mild jetlike axial Mach number profile has been shown to exist.[9]

The notion that a chamfered tip reduces losses was explored further by examining existing pitot pressure data. When the minimum pitot pressures in the cores are normalized by the freestream values and plotted against t/c for models with squared-off tips, data from various sources show trends that are reasonably characterized by simple power laws (Figs. 3a and 3b).[2,3,5,6,10] However, when the present chamfered tip results are superimposed on the same graphs, they show a milder pitot pressure ratio drop than that given by the curve fits to the squared-off tip data. It is suggested that the normalized pitot pressure in the center of a vortex generated from a chamfered wing tip corresponds to that produced by a squared-off wing having a smaller t/c. In other words, using the normalized pitot pressure in the core as an indicator, it seems established that chamfering the tip has the same effect as reducing the t/c of a wing; that is, it would reduce the losses related to

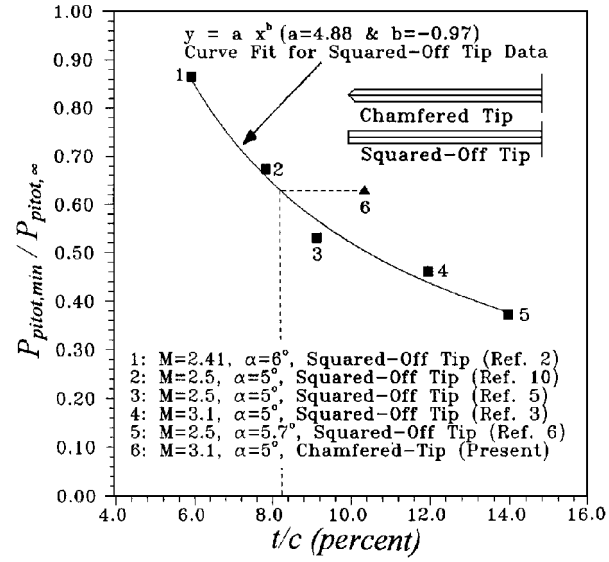

a) 5 deg $\leq \alpha \leq$ 6 deg

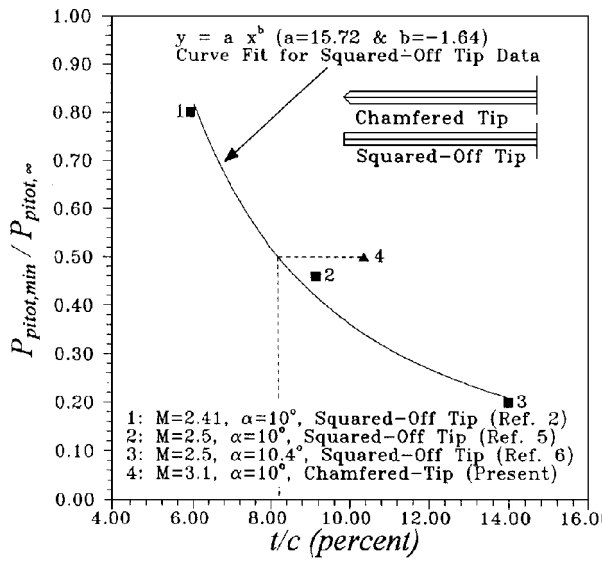

b) 10 deg $\leq \alpha \leq$ 10.4 deg

Fig. 3 Normalized minimum pitot pressure readings in the vortex cores correlated with thickness to chord ratios for squared-off and chambered wing tips.

crossflow separation during vortex generation thereby diminishing axial flow retardation in the near field. However, as the tip vortex convects farther downstream and dissipative effects and circulation continue to compete, a different axial flow profile in the core from the one obtained in the near field may ultimately develop so that it is possible that there would be a different axial flow profile but not necessary.

Although the vortex properties have been estimated by neglecting the swirl component of velocity, it is possible to recover some swirl information from the radial momentum equation[5]

$$w^2=\frac{r}{\rho}\frac{\mathrm{d}p}{\mathrm{d}r} \tag{2}$$

For the present study, a linear fit between points from Fig. 2 was used in calculating the swirl from Eq. (2). The resulting normalized swirl profiles are shown in Fig. 4, and their resemblance to the classical incompressible Burgers' profile[5,6] is apparent. The values of maximum swirl angle, defined as $\tan^{-1}(w_{\max}/V_\infty)$, are 7.8 ± 1.8 and $= 12.4 \pm 1.8$ deg for $\alpha = 5$ and 10 deg, respectively. These values are small compared to those typically reported for low-speed wing tip vortices at the same angles of attack, which is consistent with physical intuition in that it is difficult to generate large swirl angles in a high supersonic stream.

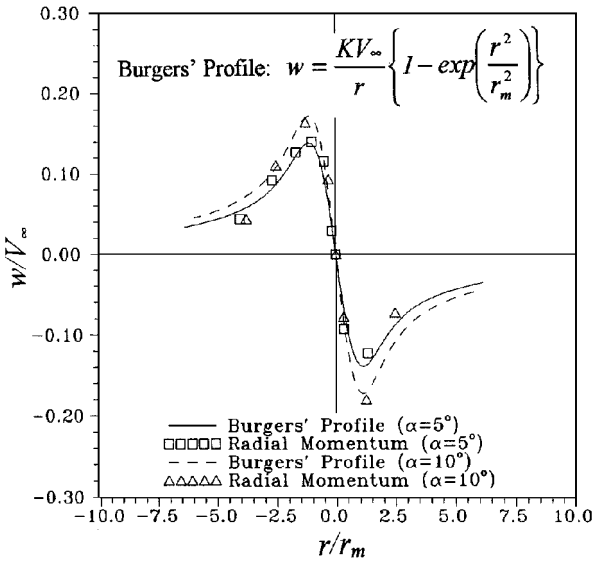

Fig. 4 Vortex swirl velocity profile; K and r_m are the characteristic strength and radius of the Burgers' vortex, respectively.

Conclusion

Results of a near-field wind-tunnel investigation on supersonic tip vortices generated by a straight wing with a sharp chamfered tip have been documented. Time-averaged positions, Mach number, velocity, and thermodynamic properties of the tip vortices were inferred from pitot pressure distributions and shadowgraph flow visualization. The tip vortices have approximately constant axial Mach number, convect downstream with very little radial diffusion of tangential momentum, and have a swirl velocity distribution reasonably described by Burgers' profile. This diffusion suppression quality of the organized structure of the tip vortex may result in the transport of entrained passive contaminants to larger downstream distances than usual wake processes would suggest, which could have significant implications in the design and operation of supersonic transports and/or affect the stealthiness of supersonic designs. A correlation is found to exist between t/c of the wings and the axial Mach number profiles in the cores. It is postulated that chamfering reduces the severity of the crossflow separation pattern around the wing tip, thereby reducing the losses associated with vortex generation. It appears possible then to modify supersonic tip vortices in the near field by simple means such as chamfering the wing tips, a concept that could be valuable in hypervelocity scramjet research where streamwise vortices are being investigated for supersonic mixing augmentation.

Acknowledgments

The assistance provided by R. J. Cresci, I. Kalkhoran, and L. Orlick is gratefully acknowledged.

References

[1]Davis, T., "The Measurement of Downwash and Sidewash Behind a Rectangular Wing at a Mach Number of 1.6," *Journal of the Aeronautical Sciences*, Vol. 19, No. 5, 1952, pp. 329–332 and 340.

[2]Adamson, D., and Boatright, W. B., "Investigation of Downwash, Sidewash and Mach Number Distribution Behind a Rectangular Wing at a Mach Number of 2.41," NACA Rept. 1340, 1957.

[3]Kalkhoran, I. M., Sforza, P. M., and Wang, F. W., "Experimental Study of Shock-Vortex Interaction in a Mach 3 Stream," AIAA Paper 91-3270, Sept. 1991.

[4]Wang, F. Y., and Sforza, P. M., "An Exploratory Wind Tunnel Study of Supersonic Tip Vortices," AIAA Paper 93-2923, July 1993.

[5]Wang, F. Y., "A Wind Tunnel Study of Supersonic Vortical Wakes from Tip Vortex Generators," Ph.D. Dissertation, Dept. of Aerospace Engineering, Polytechnic Univ., Brooklyn, NY, June 1994.

[6]Smart, M. K., Kalkhoran, I. M., and Bentson, J., "Measurements of Supersonic Wing Tip Vortices," *AIAA Journal*, Vol. 33, No. 10, 1995, pp. 1761–1768.

[7]Batchelor, G. K., "Axial Flow in Trailing Line Vortices," *Journal of Fluid Mechanics*, Vol. 20, Pt. 4, 1964, pp. 645–658.

[8]Rizzetta, D. P., "Numerical Investigation of Supersonic Wing-Tip Vortices," *AIAA Journal*, Vol. 34, No. 6, 1996, pp. 1023–1028.

[9]Ganzer, U., and Szodruch, J., "Vortex Formation over Delta, Double-Delta and Wave Rider Configurations at Supersonic Speeds," AGARD-CP-428, Nov. 1987, pp. 25.1–25.32.

[10]Wang, F. Y., Sforza, P. M., and Pascali, R., "Vortex-Wake Characteristics of a Supersonic Transport Wing Planform at Mach 2.5," *AIAA Journal*, Vol. 34, No. 8, 1996, pp. 1750–1752.

P. R. Bandyopadhyay
Associate Editor

Broadband Vibration Damping Using Highly Distributed Tuned Mass Absorbers

J. A. Zapfe*
Kinetic Systems, Inc., Boston, Massachusetts 02131
and
G. A. Lesieutre†
Pennsylvania State University, University Park, Pennsylvania 16802

Introduction

THE constrained layer damping treatment is a popular strategy used to control vibration in aerospace structures. The constrained layer treatment is a strain-based system in the sense that it requires dynamic strain in the base structure to function effectively. In situations where the vibratory motion does not produce significant levels of dynamic base strain, strain-based treatments can be ineffective. Sato et al.[1] examined the effect of both tensile and compressive loads on the transverse vibration of beams with constrained layer damping. The authors demonstrated, both analytically and experimentally, that the modal loss factors could be significantly reduced by in-plane tensile loads.[1] The transverse vibration of pressurized shells and the transverse vibration of helicopter rotor blades are two aerospace examples of dynamic structures that experience substantial in-plane loads in operation.

Unlike strain-based treatments, inertial dampers respond to the motion of the structure, regardless of whether or not that motion produces base strain. The classical inertial damper is a tuned mass absorber, as presented by Nashif et al.[2] Tuned mass absorbers are discrete devices that are typically effective over a very narrow frequency band. The effective band can be broadened somewhat by introducing dissipation into the spring material. The effective band can be widened still further by combining a number of absorbers, each tuned to a slightly different frequency, into a distributed system.

Several authors have examined inertial dampers distributed either in space or in frequency. Nashif et al.[2] examined the effect of distributed dampers on beams, whereas Smith et al.[3] analyzed the transverse vibration of flat plates with distributed tuned absorbers. Igusa and Xu[4] showed, on a single-degree-of-freedom base structure, how multiple tuned mass absorbers tuned to different frequencies could provide broadband energy dissipation.

The analysis of tuned mass systems, distributed both spatially and in frequency is a more recent area of research. In the context of fuzzy structures, Pierce et al.[5] used a distribution of spring/mass systems to model a plate with internal attachments. The authors showed how,

Presented as Paper 96-1595 at the AIAA/ASME/ASCE/AHS/ASC 37th Structures, Structural Dynamics, and Materials Conference, New Orleans, LA, April 15–17, 1996; received June 24, 1996; revision received Nov. 19, 1996; accepted for publication Nov. 20, 1996.

*Advanced Development Manager, 20 Arboretum Road. Member AIAA.
†Associate Professor, Department of Aerospace Engineering. Associate Fellow AIAA.